EXPERIMENTAL INVESTIGATION OF THE PLANCK LFI RECEIVER DESIGN: RESULTS FROM A 44 GHZ PROTOTYPE RECEIVER

Peter Meinhold, University of California at Santa Barbara
Michael Seiffert, Jet Propulsion Laboratories
Philip Lubin, University of California at Santa Barbara
Jeffery Childers, University of California at Santa Barbara

ABSTRACT

The Planck Surveyor LFI (Low Frequency Instrument) receiver is a pseudo-correlation or continuous comparison radiometer, the design of which has been optimized for reduction of 1/f type noise, high bandwidth, and high sensitivity. We have built a prototype receiver at 44 GHz to test the design and to investigate important tradeoffs in optimizing the system. The prototype incorporates elements from the front end through the detectors, DC signal processing, and data acquisition: each segment has been important in furthering our understanding of the requirements of the LFI receivers. To date we have demonstrated a knee frequency of 10 mHz with a bandwidth of 2.2 GHz. We describe the design of this prototype, present data indicative of its current performance, and discuss future plans.

1.0 INTRODUCTION

The Low Frequency Instrument (LFI) on the Planck Surveyor satellite is a set of High Electron Mobility (HEMT) amplifier based receivers operating in bands at 30, 44, 70 and 100 GHz. The mission goal is a noise limited nearly full sky map, built up of circular scans on the sky. The scan period will be 1 minute, so the requirement on the stability of the LFI receivers is a 1/f 'knee' frequency (F_k) around 10 mHz (f_k is defined to be the frequency at which the noise contribution from the amplifier instability is equal to the white noise contribution). The receiver design for LFI is of the 'pseudo-correlation' or 'continuous comparison' type, which has been used for over 30 years (Blum 1959, Colvin 1961, Faris 1967). The principal advantages of this type of receiver over a similar Dicke-switched system are wider bandwidth and higher sensitivity. Detailed discussion of the reasons for choosing this design and a theoretical exploration of it's fundamental operation can be found in Bersanelli, 1996, and Seiffert, 1998. A schematic diagram of the receiver planned for the Planck LFI shown in figure 1.

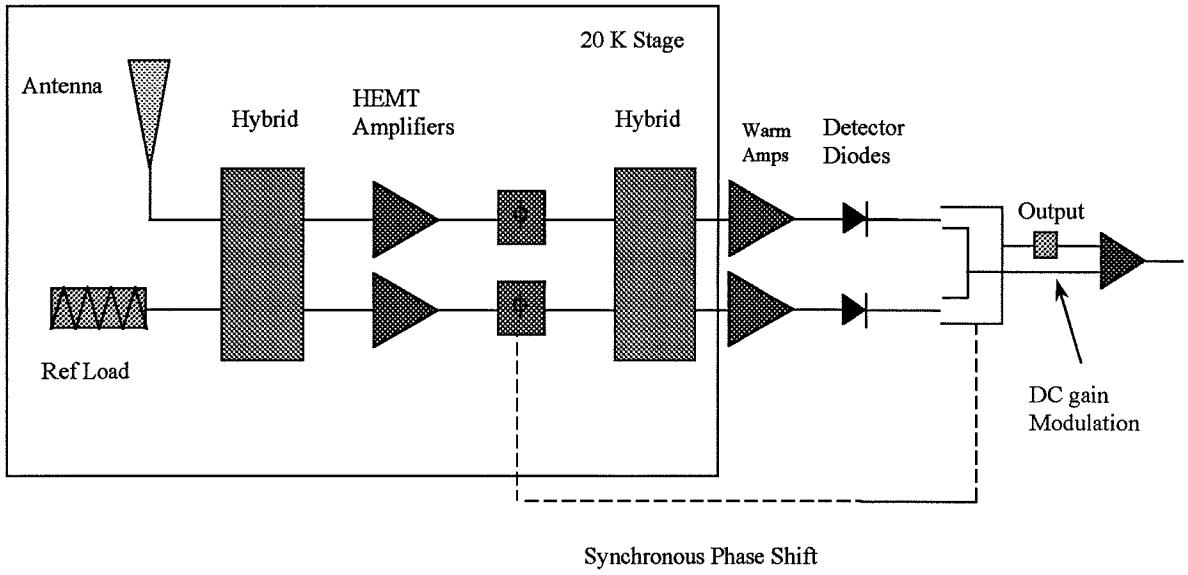

Figure 1: Shown is a schematic diagram of the Planck LFI receiver concept. The receiver minimizes the effect of gain fluctuations in the amplifiers.

The radiometer has two inputs. One input is coupled to a reference load while the other input is one polarization from a feed horn which views the sky through the Planck telescope. These two signals pass through a 180 degree hybrid coupler on to two "legs" of the radiometer. Each of these legs contains amplification and a phase shifter. The signals in the two legs are then recombined in a second hybrid coupler. The two output signals of the hybrid are thus separated back into a sky signal and a reference load signal. Which output contains the sky signal and which contains the reference load depends on the phase state set by the phase shifters. A net phase shift of 180 degrees swaps the sky signal and reference signal at the

outputs of the second hybrid. After the second hybrid the two signals pass through stainless steel wave-guide (for the high frequency channels) or semi-rigid coax (for the low frequency channels) to the warm back-end section. The signals are amplified further, pass through a band-pass filter and are converted to DC voltages by detector diodes. The voltage measured at each of the two detector diodes is of the form:

$$V_d(t) = \frac{a}{2}\left[\left(\frac{x+y}{\sqrt{2}} + n_1\right)g_1 \pm \left(\frac{x-y}{\sqrt{2}} + n_2\right)g_2\right]^2$$

Here, x(t) is the noise voltage at the sky horn, y(t) is the noise voltage of the reference load, $n_1(t)$ and $n_2(t)$ are the noise voltages contributed by the amplifiers, g_1 and g_2 are the voltage gains of the two amplifiers, the plus(minus) sign indicates 0 or 180 degree net phase shift from the phase shifter, and the diodes are assumed to be perfect square law detectors with a constant of proportionality of a. Note that the two diodes are complementary, with a fixed net phase shift of 180 degrees. When the gains g_1 and g_2 are matched, and assuming $n_1=n_2$ for simplicity, we obtain:

$$V_d(\Phi=0) = ag^2(x^2 + \frac{n_1^2+n_2^2}{2})$$

and

$$V_d(\Phi = 180) = ag^2(y^2 + \frac{n_1^2+n_2^2}{2})$$

Where we have now ignored cross terms in noise voltage, since they are uncorrelated and average to zero. Noting that here $x^2=kT_x\beta$, we can cast this result in terms of the input temperature to get :

$$V_d(\Phi = {}^{0}\!/_{180}) = ak\beta g^2(T_{x/y} + T_n)$$

Here, T_n is the average noise temperature of the amplifiers, β is the effective bandwidth, k is Boltzmann's constant. Thus the output of the radiometer in each phase switch state reflects the temperature at one of the inputs in addition to the average noise temperature of the amplifiers. In the case of the LFI, one input will be directed at the sky through the telescope, while the other will connected to a termination (a free space 4.5 K load in the case of the 100 GHz radiometers). To use this topology as a differential radiometer, we may either difference the outputs of the two diodes, or we may modulate the phase switch at a high rate (500 Hz or more) and difference successive measurements of each diode. In either case, in order to null the system and minimize the 1/f noise contribution, we need to multiply one of the states by a constant, shown (Seiffert 1998) to be:

$$r = \frac{T_x + T_n}{T_y + T_n}$$

We have chosen to use successive differences on each diode, minimizing the 1/f contributions of the detector diodes, warm amplifiers, and reducing our sensitivity to back end temperature gradients etc. Thus our final radiometer output looks like:

$$V = V_d(\Phi = 0) - rV_d(\Phi = 180) \propto T_x - T_y$$

In practice, we perform this difference in software, giving us more control over the value of r, and information about the 1/f characteristics of the individual phase states before differencing. Seiffert (1998) gives an expression for the 1/f knee frequency of the radiometer:

$$f_k = \frac{A^2\beta}{8}(1-r)^2\left(\frac{T_n}{T_n+T_x}\right)^2$$

A is a number describing the intrinsic stability of the amplifiers, and has a value of $1.8\text{x}10^{-5}$ for the 5 stage 44 GHz amplifiers discussed below.

2.0 THE 44 GHz PROTOTYPE

2.1 Goals

Our principal goal in buiding the prototype is to verify the theoretical operation of the radiometer, down to the very low f_k required by the LFI. In addition, we would like to investigate the sensitivity of the system to various systematic effects, such as temperature drift in backend components etc. In the process of making the system work, we have gained important information about the appropriate way to aquire and analyse the data, in addition to valuable information about individual components.

2.2 Radiometer Construction

Figure 2 shows the layout of our test radiometer, constructed of (mostly) parts available in our lab at UCSB. Cooling is accomplished with a liquid Helium dewar equipped with vacuum feed thrus for the waveguides. There are a few differences between figure 1 and figure 2. We are using only 1 phase shifter. The second hybrid amplifier is warm, and we have inserted variable attenuators in each leg. This allows us easy access to the phase matched legs of the radiometer, primarily in order to perform gain match using both the amplifier bias and an attenuator, and phase match using shims at a wave-guide interface. One input is coupled to a temperature controlled wave-guide load, the other is coupled to an identical load with a cross-guide coupler. The cross-guide is realized in stainless wave-guide for thermal isolation between the cold radiometer and the warm section, and provides a –38 dB coupling value to a vacuum feed-through, used to inject signals from the vector network analyzer (HP 8510C). This input configuration allows us to tune the gain and phase match with the network analyzer, then remove the analyzer and operate the radiometer with the controllable thermal loads to investigate noise and 1/f at different load temperatures and differences, all with the cold amplifiers operating at cryogenic temperatures.

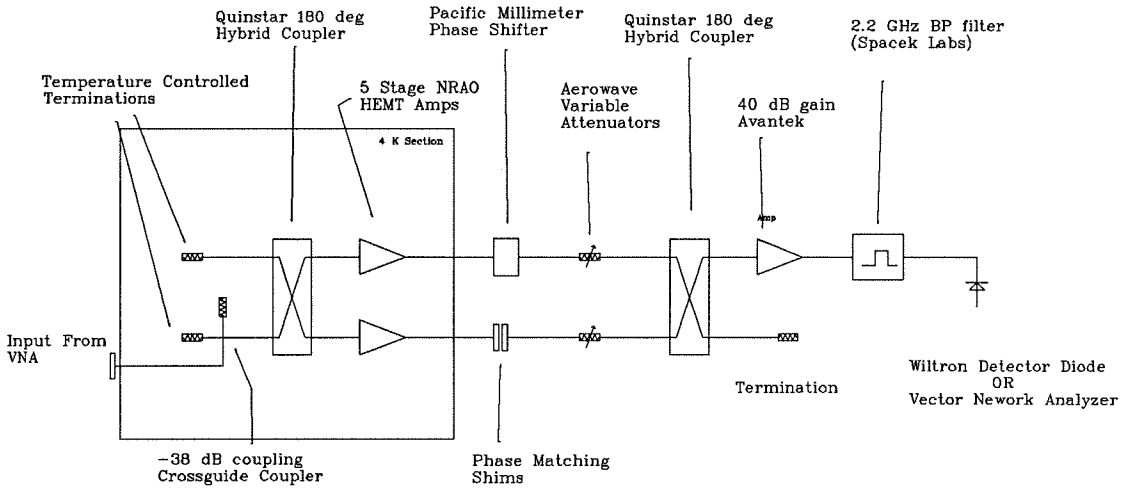

Figure 2. Schematic of the Prototype Radiometer. Note differences from figure 1, particularly division of phase sensitive section between warm and cold parts, and the low coupling value cross-guide at one input for VNA signal injection.

The cryogenic amplifiers are an NRAO design, constructed with discrete devices: 1 stage of InP HEMT from Hughes, 4 stages of GaAs HEMT from Starcomm. The 180 degree hybrid couplers are from Quinstar and the 0/180 degree phase switch is from Pacific Millimeter. The detector diode is a Wiltron 75KC50, and the attenuators are from Aerowave. The warm amplifier (from Avantek) has a gain of approximately 40 dB, and we have a 2.2 GHz wide iris filter from Spacek Labs. We use this filter to define our bandwidth, and to give us a smaller range over which to match our two amplifiers (as the amps were not expressly designed to be identical). The input terminations are made of Eccosorb (cr117), machined to a very fine point and inserted into stainless steel waveguide sections. A small temperature sensor is inserted directly into the Eccosorb, and the temperature of the load is determined by balancing cooling from a copper strap to the 4 K plate with input power to a heater resistor attached to the load. The loads have better than –35 dB return loss.

2.3 Balancing

With the system connected to the VNA, we match the gain and phase of the two legs of the radiometer. This is done by first biasing only one of the cold HEMT amplifiers and measuring the system gain. Then we bias only the other amplifier and measure the gain difference. By tuning bias settings and attenuation in the two legs, we can generally get the gain matched within 1 dB across our 2.2 GHz band-pass. The same procedure is then followed for the phase match, where tuning is accomplished by inserting shims of different thickness at a wave-guide joint in one leg of the radiometer. Phase match across the band of ±10 degrees is relatively easy to obtain. The next step is to measure the 'isolation' of the system, where we measure the difference between the radiometer output in the phase state looking at the termination, and the output

while looking at the VNA. This is indicative of the overall gain/phase match of the system, generally we achieve between –20 and –25 dB isolation.

Our phase switch has an important asymmetry, which is that the loss in the two states is not identical for identical bias currents. Normally the switch is run at +20 or –20 mA for the two states, this can result in differential loss of order .2 dB. Since the phase switch is the one portion of the system which is not modulated by the phase switching, it is critical to balance the loss in the two states. We do this by observing the radiometer output (using the detector diode) with only thermal loads connected and only the amplifier in the phase switching leg biased. We then tune the phase switch bias currents to make the output equal in both phase states (luckily this does not adversely affect the phase switching). Only after this is done do we perform the gain and phase balancing described in the previous paragraph. It is crucial to do this loss balancing to get the full performance from the system: we gained nearly an order of magnitude reduction in 1/f knee by this loss balancing.

2.4 Data Acquisition

As mentioned above, we take data from this radiometer by sampling only 1 detector. We require high gain, an ideal integrator, and sampling synchronous with the phase switch state. We choose to sample at 1 kHz, switching the phase at 500 Hz. We have built an analog front end and synchronous sampling system for this work and for a balloon payload. The analog section consists of a x10 low noise preamp, a switchable gain stage (x1-x100) followed by a dc offsetting circuit. We minimize the DC component of the signal going into the integrator to increase our dynamic range. The integrator is a Burr-Brown IVC-102, and is followed by a sample and hold circuit. The output of the sample and hold and the preamp section are brought out through linear opto-isolator amplifiers (CP Clare LIA100). A separate timing board synchronizes the sample and hold and integration/reset in addition to the phase switch signal. In general, the gain switching in the second stage of pre-amplification is used to set the dynamic range, rather than to null the output, we have been able to do the nulling all in software. The procedure is to acquire 600+ seconds of data sampled at 1 kHz, then to separate out the 0 phase state samples from the 180 phase state samples. We then calculate power spectra for these data sets and find the value of r by comparing the white noise levels. The white noise of the detector in a given phase switch state is given by:

$$\Delta T = \sqrt{2}\frac{(T_x + T_n)}{\sqrt{\beta\tau}}$$

which is a modification to the standard radiometer equation, including an extra factor of $\sqrt{2}$ due to the 50% duty cycle of one switch state. Thus r is equal to the ratio of the white noise levels in the individual phase states. We previously used AC coupling between the preamp and the integrator to increase our dynamic range, but found that in order to properly calculate and apply the correct value of r, it was necessary to replace the AC coupling with a DC offset circuit as shown: unless the AC time constant is longer than the time-scale of interest (i.e. 100 seconds or so), information will be lost, and the subtraction will be incorrect on time-scales longer than the coupling time constant.

3.0 RESULTS

3.1 Data

Figure 3 shows the power spectra from the two phase states superimposed, in the case of a relatively large offset of 13 K, along with the difference power spectrum. Note that we use the term power spectrum loosely, as we generally plot the square root of the power spectrum in order to make the units more useful. We have smoothed the curves to bring out the difference in white noise level due to the two different load temperatures, and used the known load temperatures to calibrate the data in temperature units. The white noise levels imply amplifier noise temperatures of around 40 K, and are consistent with the bandwidth of 2.2 GHz. The load temperatures are 20 K and 7 K.

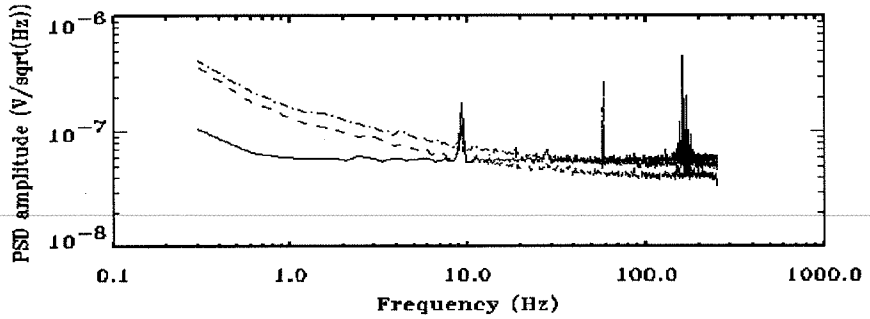

Figure 3. We display the power spectra from the two phase states and the difference data power spectrum for the case of large offset. The dash-dot line is tha phase viewing the 20 K termination, the dash line is the phase viewing the 7 K termination, and the solid line is the difference data. The effective knee frequency for the undifferenced data is around 10 Hz.

Figure 4 shows an expanded plot of the power spectrum of the difference data set from figure 4, in addition to a difference power spectrum from a data set with offset smaller than 1 K. The difference in the knee is evident, particularly from the fits, which give 30 mHz for the 13 K offset curve and 12 mHz for the 1 K offset. Note that these fits do not give spectral indices of –1 for the low frequency part of the power spectra (although the undifferenced outputs do give very close to –1). This may be evidence that we are now limited by more than one 1/f type noise contributions with different knee frequencies and amplitudes.

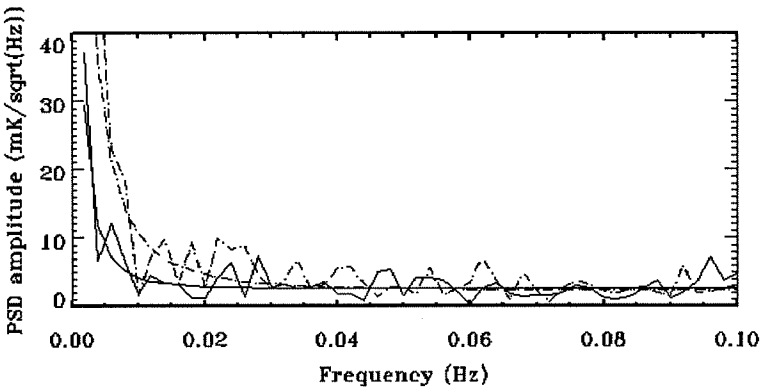

Figure 5. Shown is an expanded view (linear in both axes) of the relevant portion of the power spectrum of the differenced data. The solid line is from the small offset case and the dotted line is from the larger (13K) offset case along with fitted curves. Note this plot is calibrated in temperature units.

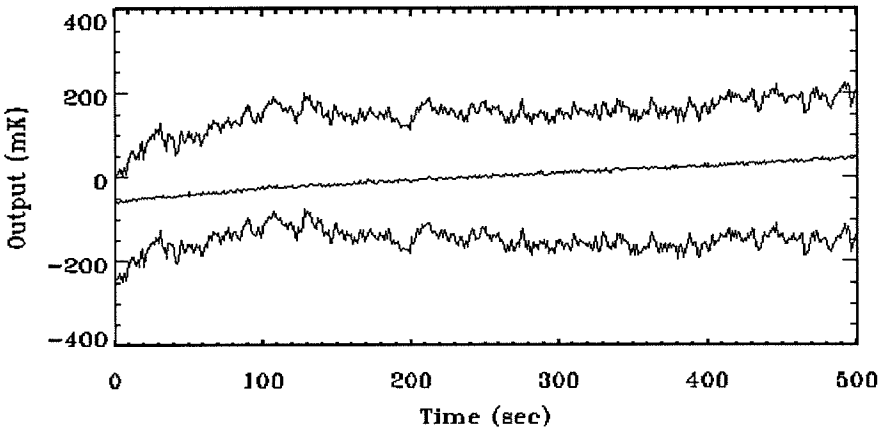

Figure 6. Time ordered data are plotted to illustrate the radical reduction in noise. The upper line shows the data from the 0 degree phase state, the lower line is the data from the 180 degree phase state, and the center line is the difference data. All data have been smoothed to 1 second to illustrate the 1/f noise component, the termination temperatures were within 1 K of each other.

3.2 Discussion

Referring to equation 6, we find that for these offsets and bandwidth, we should expect f_k~1 mHz for the 13 K offset case, and close to zero for the low offset case. The reasons for not reaching the theoretical stability are not fully understood. There are a number of effects which need to be controlled carefully on these extreme timescales, particularly thermal and mechanical stability of the warm, phase sensitive section of our test radiometer. We have done a limited amount of temperature control on the most sensitive elements (the phase shifter and detector diode in particular), with some success, but in order to reach past 10 mHz, it may be necessary to put the entire radiometer (at least to the second hybrid coupler) in a vacuum environment with temperature control on all parts of the system. Of course in the LFI flight configuration, all of the phase sensitive parts will be in a single housing, cooled to 20 K and kept far more thermally and mechanically stable than we can achieve with our current setup, so our results are extremely promising for future, more integrated realizations of the system.

Our phase shifter may currently be the limiting element in the prototype: Tests done on the phase shifter stability alone indicate that the differential loss may vary by several parts in 10^5 on a time scale of 100 seconds (10 mHz). Of course the specific design and devices used to produce our phase shifter are different than those that will be used in the final LFI design, and 10 mHz is well below the spin rate of the spacecraft, so it is unlikely that this will cause a problem for the instrument.

4.0 FURTHER WORK

4.1 Sensitivity and Bandwidth

Currently the system noise temperature is 40 K, adequate for testing the concept, but a factor of 2-3 higher than expected given the past performance of these amplifiers. There are several likely reasons for this excess noise which we will be sorting out in the next round of testing. The most likely problems are associated with simple optimization of the HEMT conditions for noise. To date, we have ignored bias tuning for noise while we tuned for gain and phase match between the amplifiers. Simultaneous tuning for noise and match is the next step, along with the addition of light on the devices, important for these amplifiers (again, this is not relevant for LFI). We will also be testing for stability as a function of bandwidth. With more optimum HEMT noise and wider bandwidth, the system will have noise and other parameters closer to the expected LFI performance.

4.2 Match requirements

So far we have matched gain and phase as well as practical. Noise temperature match of the HEMT amplifiers is also important. We plan to make improved measurements of the amplifier noise temperatures and simultaneously match gain, phase and noise, while minimising the overall noise temperature. We then plan to determine the output stability as a function of the noise, phase and gain match by varying them. This will provide crucial input to the design of the flight radiometers.

5.0 CONCLUSION

We have demonstrated extremely good stability performance in a prototype realization of the Planck LFI radiometer design. Tests have raised a number of issues to be pursued for optimum performance. It appears a significant but straightforward effort will result in the development and production of flight radiometers meeting the LFI requirements.

REFERENCES

1. Bersanelli et al., 1996. *ESA, COBRAS/SAMBA Report on the Phase A Study,* D/SCI(96)3.
2. Blum, E. J., 1959, *Annales d'Astrophysique*, 22-2,140.
3. Colvin, R.S., 1961, Ph.. Thesis, Stanford University.
4. Faris, J.J., 1966, *J. Res NBS*, **71C**, No. 2, 153.
5. Seiffert, M. et al, *Rev. Sci. Instrum.*, submitted 1997.